Long period grating resonances in photonic bandgap fiber

P. Steinvurzel, E. D. Moore[1], E. C. Mägi, B. T. Kuhlmey, and B. J. Eggleton

ARC Centre for Ultrahigh-bandwidth Devices for Optical Systems (CUDOS)
School of Physics A28, University of Sydney, NSW 2006 Australia
[1]*also with Dept. of Electrical and Computer Engineering, University of Colorado, UCB 440, Boulder, CO 80309*
pes@physics.usyd.edu.au

http://www.physics.usyd.edu.au/cudos

Abstract: We demonstrate the formation of stress-induced long period gratings (LPGs) in fluid-filled photonic bandgap fiber (PBGF). Based on our experimental results, simulations, and theoretical understanding of LPGs, we identify coupling to a guided LP_{11}-like mode of the core and lossy LP_{1x}-like modes of cladding microstructure for a single grating period. The periodic modal properties of PBGFs allow for coupling to the same mode at multiple wavelengths without being near a dispersion turning point. Simulations identify inherent differences in the modal structure of even and odd bands.

OCIS codes: (060.2310) Fiber optics; (050.2770) Gratings; (230.3990) Microstructure devices

References and links

1. A. M. Vengsarkar, P. J. Lemaire, J. B. Judkins, V. Bhatia, T. Erdogan and J. E. Sipe, "Long Period Fiber Gratings as Band Rejection Filters," J. Lightwave Technol. **14**, 58-65 (1996).
2. A. M. Vengsarkar, J. R. Pedrazzani, J. B. Judkins, P. J. Lemaire, N. S. Bergano and C. R. Davidson, "Long-period fiber-grating-based gain equalizers," Opt. Lett. **21**, 336-338 (1996).
3. C. D. Poole, J. M. Wiesenfeld, D. J. Digiovanni and A. M. Vengsarkar, "Optical Fiber-Based Dispersion Compensation Using Higher-Order Modes Near Cutoff," J. Lightwave Technol. **12**, 1746-1758 (1994).
4. V. Bhatia and A. M. Vengsarkar, "Optical fiber long-period grating sensors," Opt. Lett. **21**, 692-694 (1996).
5. B. J. Eggleton, P. S. Westbrook, R. S. Windeler, S. Spälter and T. A. Strasser, "Grating resonances in air-silica microstructured optical fibers," Opt. Lett. **24**, 1460-1462 (1999).
6. B. J. Eggleton, P. S. Westbrook, C. A. White, C. Kerbage, R. S. Windeler and G. L. Burdge, "Cladding-mode-resonances in air-silica microstructure optical fibers," J. Lightwave Technol. **18**, 1084-1100 (2000).
7. J. C. Knight, "Photonic crystal fibres," Nature **424**, 847-851 (2003).
8. A. Diez, T. A. Birks, W. H. Reeves, B. J. Mangan and P. St. J. Russell, "Excitation of cladding modes in photonic crystal fibers by flexural acoustic waves," Opt. Lett. **25**, 1499-501 (2000).
9. M. D. Nielsen, G. Vienne, J. R. Folkenberg and A. Bjarklev, "Investigation of microdeformation-induced attenuation spectra in a photonic crystal fiber," Opt. Lett. **28**, 236-8 (2003).
10. J. H. Lim, K. S. Lee, J. C. Kim and B. H. Lee, "Tunable fiber gratings fabricated in photonic crystal fiber by use of mechanical pressure," Opt. Lett. **29**, 331-333 (2004).
11. K. Morishita and Y. Miyake, "Fabrication and resonance wavelengths of long-period gratings written in a pure-silica photonic crystal fiber by the glass structure change," J. Lightwave Technol. **22**, 625-630 (2004).
12. J. Kim, G.-J. Kong, U.-C. Paek, K. S. Lee and B. H. Lee, "Demonstration of an Ultra-Wide Wavelength Tunable Band Rejection Filter Implemented with Photonic Crystal Fiber," IEICE Trans. Electron. **E88-C**, 920-924 (2005).
13. G. Kakarantzas, T. A. Birks and P. St. J. Russell, "Structural long-period gratings in photonic crystal fibers," Opt. Lett. **27**, 1013-15 (2002).
14. G. Humbert, A. Malki, S. Fevrier, P. Roy and D. Pagnoux, "Electric arc-induced long-period gratings in Ge-free air-silica microstructure fibres," Electron. Lett. **39**, 349-350 (2003).
15. Y. Zhu, P. Shum, H. J. Chong, M. K. Rao and C. Lu, "Strong resonance and a highly compact long-period grating in a large-mode-area photonic crystal fiber," Opt. Express **11**, 1900-1905 (2003), http://www.opticsexpress.org/abstract.cfm?URI=OPEX-11-16-1900.
16. H. Dobb, K. Kalli and D. J. Webb, "Temperature-insensitive long period grating sensors in photonic crystal fibre," Electron. Lett. **40**, 657-658 (2004).
17. X. W. Shu, X. M. Zhu, Q. L. Wang, S. Jiang, W. Shi, Z. J. Huang and D. X. Huang, "Dual resonant peaks of $LP_{0,15}$ cladding mode in long-period gratings," Electron. Lett. **35**, 649-651 (1999).

#10342 - $15.00 USD Received 17 January 2006; revised 9 March 2006; accepted 16 March 2006

18. V. Grubsky and J. Feinberg, "Long-period fiber gratings with variable coupling for real-time sensing applications," Opt. Lett. **25**, 203-205 (2000).
19. Z. Y. Wang and S. Ramachandran, "Ultrasensitive long-period fiber gratings for broadband modulators and sensors," Opt. Lett. **28**, 2458-2460 (2003).
20. R. T. Bise, R. S. Windeler, K. S. Kranz, C. Kerbage, B. J. Eggleton and D. J. Trevor, "Tunable photonic bandgap fiber," in *Optical Fiber Communications Conference*, Post Conference vol. 70 of OSA Trends in Optics and Photonics Series Technical Digest (Optical Society of America, Washington, D.C., 2002), 466-468.
21. N. M. Litchinitser, A. K. Abeeluck, C. Headley and B. J. Eggleton, "Antiresonant reflecting photonic crystal optical waveguides," Opt. Lett. **27**, 1592-1594 (2002).
22. T. P. White, R. C. McPhedran, C. M. de Sterke, N. M. Litchinitser and B. J. Eggleton, "Resonance and scattering in microstructured optical fibers," Opt. Lett. **27**, 1977-1979 (2002).
23. N. M. Litchinitser, S. C. Dunn, B. Usner, B. J. Eggleton, T. P. White, R. C. McPhedran and C. M. de Sterke, "Resonances in microstructured optical waveguides," Opt. Express **11**, 1243-1251 (2003), http://www.opticsexpress.org/abstract.cfm?URI=OPEX-11-10-1243.
24. R. C. Youngquist, J. L. Brooks and H. J. Shaw, "Two-mode fiber modal coupler," Opt. Lett. **9**, 177-179 (1984).
25. S. J. Garth, "Intermodal Coupling In An Optical Fiber Using Periodic Stress," Appl. Opt. **28**, 581-587 (1989).
26. W. J. Wadsworth, N. Joly, J. C. Knight, T. A. Birks, F. Biancalana and P. St. J. Russell, "Supercontinuum and four-wave mixing with Q-switched pulses in endlessly single-mode photonic crystal fibres," Opt. Express **12**, 299-309 (2004), http://www.opticsexpress.org/abstract.cfm?URI=OPEX-12-2-299.
27. A. Argyros, T. A. Birks, S. G. Leon-Saval, C. B. Cordeiro and P. St. Russell, "Guidance properties of low-contrast photonic bandgap fibres," Opt. Express **13**, 2503-2504 (2005), http://www.opticsexpress.org/abstract.cfm?URI=OPEX-13-7-2503.
28. T. P. White, B. T. Kuhlmey, R. C. McPhedran, D. Maystre, G. Renversez, C. M. de Sterke and L. C. Botten, "Multipole method for microstructured optical fibers. I. Formulation," J. Opt. Soc. Am. B **19**, 2322-30 (2002).
29. B. T. Kuhlmey, T. P. White, G. Renversez, D. Maystre, L. C. Botten, C. M. de Sterke and R. C. McPhedran, "Multipole method for microstructured optical fibers. II. Implementation and results," J. Opt. Soc. Am. B **19**, 2331-40 (2002).
30. M. Yan and P. Shum, "Antiguiding in microstructured optical fibers," Opt. Express **12**, 104-116 (2004), http://www.opticsexpress.org/abstract.cfm?URI=OPEX-12-1-104.
31. S. Wilcox, L. C. Botten, R. C. McPhedran, C. G. Poulton and C. M. de Sterke, "Modeling of defect modes in photonic crystals using the fictitious source superposition method," Phys. Rev. E **71**, 056606 (2005).

1. Introduction

Long period gratings (LPGs) in optical fibers resonantly couple light between two copropagating modes, typically the fundamental mode and a higher order mode (HOM) of the core or cladding. LPGs have many useful device applications in optical filtering [1], gain flattening [2], mode conversion [3], and sensing [4]. However, on a more fundamental level, LPGs can be used as a diagnostic tool for probing the modes of novel fiber structures [5, 6]. The LPG phase matching condition, given by $\lambda_{res}=\Lambda|n_{eff}^{fund}- n_{eff}^{HOM}|$, where λ_{res} is the resonance wavelength, Λ is the grating period, and n_{eff}^{x} is the effective index of one of the coupled modes, depends on the effective index difference between the two coupled modes, which is typically small and thus sensitive to variations in n_{eff}^{fund} or n_{eff}^{HOM}. If Λ and n_{eff}^{fund} are known, then measuring λ_{res} can be a highly sensitive method for experimentally determining n_{eff}^{HOM}.

Microstructured optical fibers (MOFs), optical fibers with holes running down the fiber axis, have attracted a great deal of interest over the past decade in large part because of their unique and very useful modal and dispersive properties, e.g. endlessly single mode behavior, low loss guidance in air, or engineered dispersion for enhancing nonlinear processes [7]. Long period gratings have been demonstrated in solid core index guided MOFs [5, 6, 8-16], primarily in the context of fiber devices, where they have been shown to be more stable against changes in temperature, strain, or the index surrounding the fiber as compared to LPGs in step index fibers. It has also been shown that in air/silica MOFs, the beat length between the fundamental and cladding modes, equivalent to the period required for phase matching Λ, generally decreases with wavelength [8-12], contrary to the usual case in SIFs,

#10342 - $15.00 USD Received 17 January 2006; revised 9 March 2006; accepted 16 March 2006

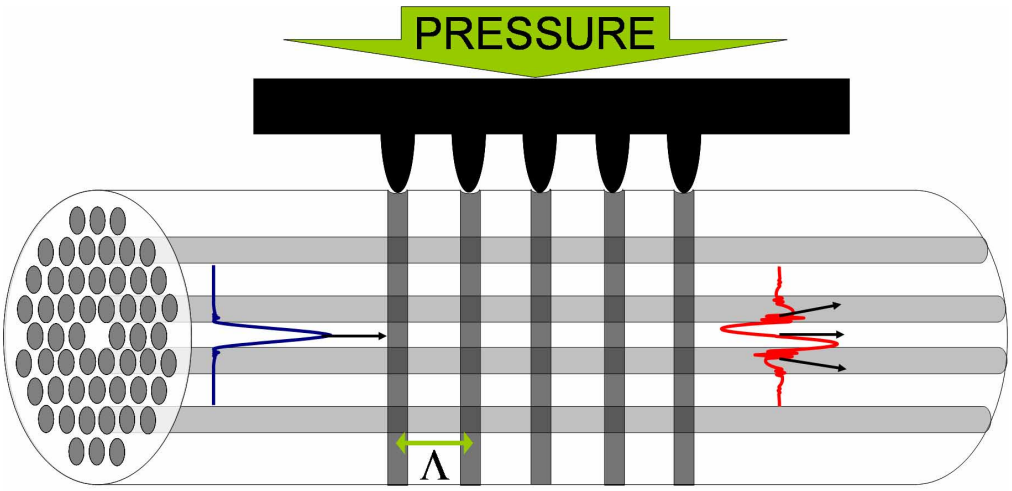

Fig. 1. Schematic diagram of solid core PBGF with mechanically-induced LPG which couples the fundamental core mode to an antisymmetric higher order mode of the fiber. Shaded vertical boxes indicate stressed regions of the fiber. In the PBGF cross-section at left of diagram, gray corresponds to high index regions and white corresponds to low index regions.

though this behavior is not unique to MOFs and can exist in SIFs for some cladding modes [17-19] (it also occurs in SIFs for coupling between two guided modes [3]).

Photonic bandgap fibers (PBGFs) are a type of MOF in which the core has a lower refractive index than the average index of the cladding microstructure [7]. Here we consider the specific case of a solid core PBGF in which the microstructure is a periodic array of identical high refractive index rods embedded in a low index background and the core is formed by a single missing rod defect. Such PBGFs of course are not air/silica fibers but rather composed of two different materials and can be fabricated by taking a solid core MOF with airholes in the cladding and filling the holes with a high index fluid [20]. In these fibers the guidance is due to anti-resonant scattering from the high index rods [21-23] and the transmission spectrum consists of discrete frequency bands. The modal properties are thus very different from index guided fibers, and this will be reflected in the LPG spectra PBGFs.

In this paper we demonstrate the first LPG in a PBGF. The grating is formed by inducing periodic mechanical stresses on the fiber [9, 10, 24, 25]. The LPG couples to HOMs of the core and the microstructure. Since the mode structure is periodic in frequency, we obtain phase matching between the fundamental mode and same higher order mode (HOM) at multiple wavelengths for a single grating period far from any dispersion turning point. We obtain very good agreement with simulations in determining the phase matching conditions. We also show that the properties of the HOMs unexpectedly depend on the parity of the transmission bands, and in particular that the odd bands support both a low loss LP_{11}-like HOM of the defect core and lossy HOMs of the microstructure, whereas the even bands support lossy HOMs of the microstructure only.

2. Experiment

The fiber used in the experiment, ESM-12-01 from Crystal Fiber A/S, is a silica MOF with 4 rings of air holes, where the holes have an average diameter of 3.51 μm arranged on a triangular lattice with an average pitch of 7.7 μm. The core is formed by a single missing rod defect. We make this fiber into a PBGF by using a vacuum pump to fill the holes with a high index fluid from Cargille Laboratories with $n_D = 1.64$. After the fiber is filled, the ends are cleaved to ensure that no fluid rests near the core on the fiber endface. We do not strip the fiber jacket in any of our measurements. Figure 2(a) (black) shows the transmission spectrum through a 10 cm length of this fiber as measured on an optical spectrum analyzer (OSA) using

#10342 - $15.00 USD Received 17 January 2006; revised 9 March 2006; accepted 16 March 2006

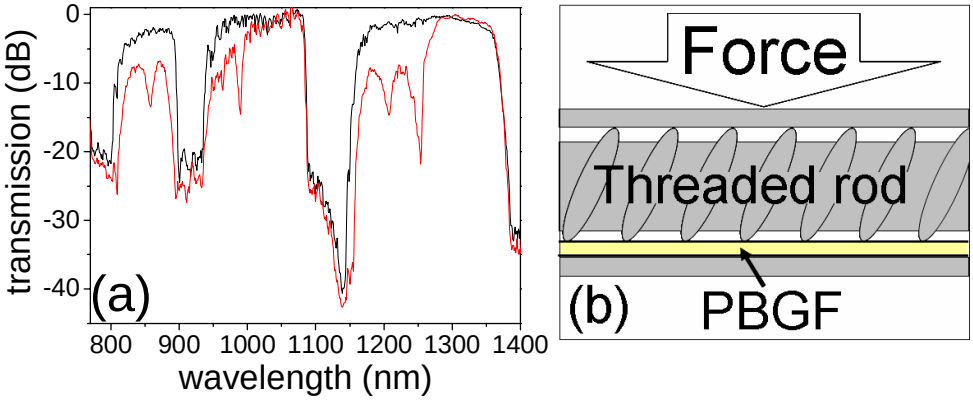

Fig. 2. (a) Transmission spectrum through length of 10 cm PBGF with no grating (black) and with a grating (red) induced by periodic stress. (b) Schematic diagram of experimental embodiment of mechanical stress grating.

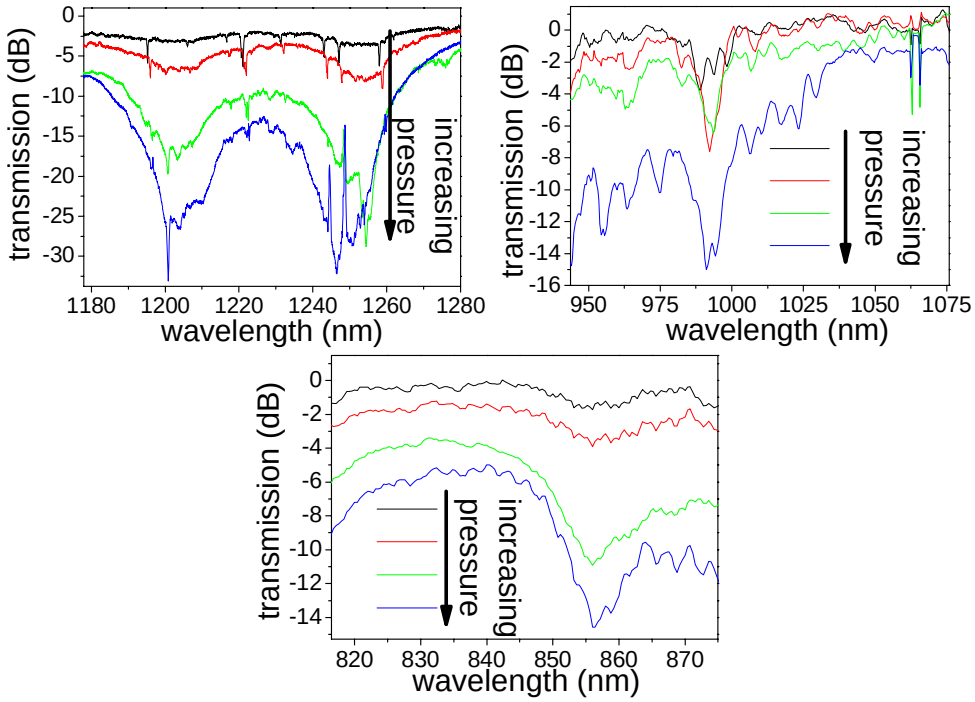

Fig. 3. Grating growth in the 4th , 5th, and 6th transmission bands for increasing applied pressure. Data in normalized with respect to transmission with no applied pressure. The grating growth at the resonances near 1250 and 1200 nm are measured using 0.2 nm resolution on the OSA, other resonances are measured using 2 nm resolution.

a supercontinuum light source [26] butt-coupled to the PBGF. We observe three discrete transmission bands. If we designate the lowest frequency transmission band supported by the fiber as the first band, then the measured bands correspond to the 4th, 5th, and 6th transmission bands of this fiber. We then form our LPG by inducing periodic stresses in the fiber. This is done by clamping the fiber into a V-groove cut in an aluminum stage and then pressing down on it with a 5 cm long threaded rod with a thread spacing of 660 μm (Fig. 2(b)). The force is applied by screwing the top plate down to fiber holder. When we apply pressure to the fiber,

#10342 - $15.00 USD Received 17 January 2006; revised 9 March 2006; accepted 16 March 2006

we observe a single loss peak in the 5th and 6th bands and two loss peaks in the 4th band. By contrast, we note that if we induce a grating in the same fiber with no fluid in the airholes, so that the modes are index guided and the transmission is broadband, we measure only a single resonance dip near 1020 nm.

The strength of the grating coupling depends on the amount of pressure applied. Figure 3 shows the growth of the resonances for increasing grating strength. The resonances near 1250 nm and 1200 nm are measured using a resolution of 0.2 nm and the other resonances are measured using a resolution of 2 nm. The sharp peaks in the high resolution scan are not yet well-understood. We also measured the temperature dependence of the LPG resonances. The refractive index of the fluid has a large thermo-optic coefficient (-4.65×10^{-4} $^{o}C^{-1}$), and so we found the resonances to be very sensitive to temperature, with tuning coefficients of -1.58 nm/^{o}C, -1.38 nm/^{o}C, -1.01 nm/^{o}C, and -0.94 nm/^{o}C for the four measured resonances going from long wavelength to short wavelength. The details of the thermal tuning characteristics of the PFBG LPG will be described in a future publication.

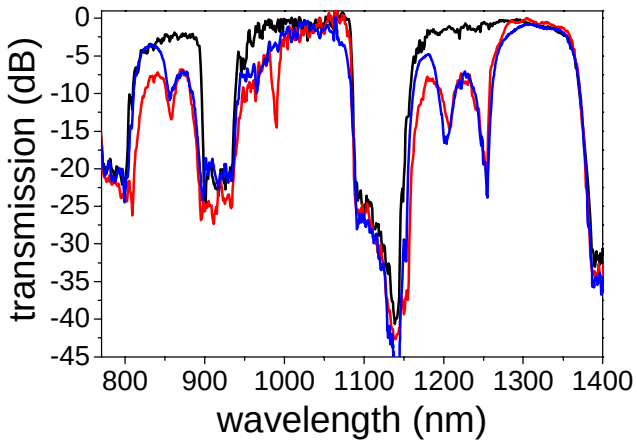

Fig. 4. Transmission spectrum through length of 10 cm PBGF with no grating (black) and with a grating (red and blue) induced by periodic stress. In the red curve, there is a slight bend of the fiber at the clamp beyond the grating region which strips out the HOMs; in the blue curve, this bend is minimized.

Finally, we note that measured spectrum was sensitive to how the fiber was clamped to the stage, away from the grating region. Since the V-groove was neither perfectly straight nor of uniform depth and width, we found that if the clamping was not done with sufficient care, the clamp would bend the free ends of the fiber upwards or sideways and we observed losses at the edges of the transmission bands, consistent with the work of Argyros et al. [27]. However, the bend can also be an advantage in that it acted as a HOM stripper. In Fig. 4 we show grating spectra with a slight bend (bend radius ~1-10 cm) at the clamp (red curve) and our best results for attempting to remove the bend (blue curve). As compared to the red curve, we note that the blue curve generally transmits better near the short wavelength edges of the transmission band edges, consistent with a reduction in bend loss [27]. More importantly, the resonance dip near 1 μm disappears, though the other resonances are relatively unaffected. This indicates that the mode we couple to at that resonance has lower propagation loss than the other HOMs, though it is still strongly susceptible to bend loss. We return to this point in Sec. 4.

3. Simulation

We simulate the modes of our PGBF using the multipole method [28, 29]. The simulations include the material dispersion effects of silica and the index high fluid. Since the mechanically induced stresses have a preferred direction, the grating coupling coefficient has

#10342 - $15.00 USD Received 17 January 2006; revised 9 March 2006; accepted 16 March 2006

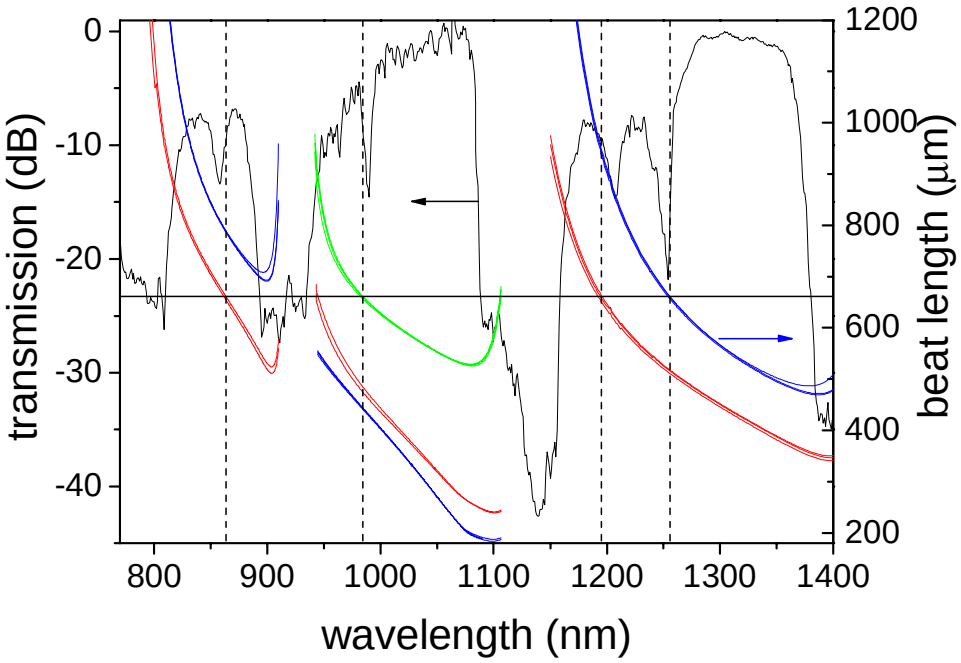

Fig. 5. Transmission spectrum of PBGF LPG (black line, left axis) and numerically simulated phase matching curves (colored lines, right axis) between fundamental and LP_{1x}-like modes. Blue and red lines correspond to LP_{11}- and LP_{12}-like modes of the microstructure, respectively, and green line corresponds to LP_{11}-like mode of the core. Vertical lines show that the phase matching curves cross the Λ=660 μm line at wavelengths extremely close to the measured resonances.

an azimuthal dependence which primarily couples from modes with n azimuthal nodes to modes with n+1 or n-1 azimuthal nodes. Experimentally, we launch light into the fundamental core mode of our PBGF, so the stress grating couples mainly to LP_{1x}–like modes [24, 25]. Our simulations show that the grating spectra do in fact satisfy the phase matching condition for coupling between the fundamental and LP_{1x}–like modes. In Fig. 5, we again plot the PGBF-LPG spectrum (black line) superimposed with the phase matching curves of our simulated modes (colored lines). Each colored phase matching curve is actually made up of three curves, corresponding to the TE_{0x}-, TM_{0x}-, and HE_{2x}-like modes which make up the LP_{11} manifold. The right y-axis corresponds to the beat length between the fundamental and HOMs, i.e. the grating period $\Lambda=\lambda/|n_{eff}^{fund} - n_{eff}^{HOM}|$ necessary for coupling at a particular wavelength. The horizontal line corresponds to the experimental period Λ=660 μm, and the

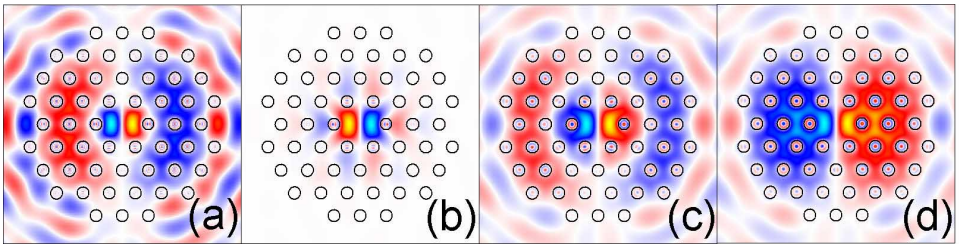

Fig. 6. Simulated transverse mode profiles of HOMs coupled by the PBGF LPG at (a) 855 nm, (b) 985 nm, (c) 1205 nm, and (d) 1250 nm. Modes (a) and (c) are LP_{12}–like modes of the microstructure, mode (b) is a LP_{11}–like mode of the core, and mode (d) is a LP_{11}–like mode of the microstructure. All plots correspond to the real part of H_y of the TM-like mode.

#10342 - $15.00 USD Received 17 January 2006; revised 9 March 2006; accepted 16 March 2006

dashed vertical lines show that at this period, the numerically simulated phase matching condition is satisfied at wavelengths which agree with the measured values to within 1%.

Figure 6 shows the simulated transverse mode profiles of the HOMs which satisfy the phase matching condition. Modes (a) and (c) have very similar field profiles (mode (c) is slightly more extended because it is at a longer wavelength and nearer to the edge of the transmission band), and we designate these as the LP_{12}-like mode of the microstructure. The fact that we can phase match to this mode at two wavelengths 350 nm apart is due to the periodic mode structure inherent to PBGFs and not to a particular dispersion turning point as required in more conventional index guiding fibers. We note that phase matching curves in the 5th band in Fig. 5 are different from those in the 4th and 6th bands, and the corresponding mode profiles in Fig. 6 are also different in the 5th band. We elaborate on this point in the following section.

4. Discussion

As mentioned above, Figs. 5 and 6 seem to indicate a qualitative difference between the 5th band and the 4th and 6th bands. Regarding the mode profiles in Fig. 6, we note that whereas modes (a), (c), and (d) appear to fill the microstructure and are quite lossy (20 dB/cm, 42 dB/cm, and 15 dB/cm, respectively), mode (b) is well confined to the core and has much lower propagation loss (0.03 dB/cm). We note that this is consistent with our finding in Fig. 4, that the LPG resonances in the 4th and 6th bands should not be sensitive to fiber bends, since the HOMs associated with these resonances have very large loss anyway, whereas the resonance in the 5th band is sensitive to bend loss because the associated HOM has relatively low propagation loss in the absence of bends. Modes (a), (c) and (d) are in fact modes of the microstructure; specifically, modes (a) and (c) are LP_{12} modes and mode (d) is an LP_{11} mode. Simulations show that these microstructure modes exist even when the defect core is replaced by a high index rod, and they can be viewed as somewhat analogous to the antiguided modes of air-silica MOFs described in the work of Yan et al. [30]. However, the microstructure has a higher average refractive index than the surrounding silica cladding, so in this case one cannot qualitatively view the entire microstructure as big core with a low effective index with antiguidance occurring at the edge of the microstructure. Rather, the guidance appears to be antiresonant in nature (periodic dispersion relation relation, higher loss near resonances of the cylinders, n_{eff} below the lowest material index), with antiresonant scattering occurring in the interstitial regions of the microstructure. Alternately, one may view these HOMs as supermodes composed of a linear combination of leaky modes (i.e., beyond cutoff) of the individual cylinders.

We also simulated the evolution of the microstructure modes as more rings of cylinders are added. The propagation loss, determined by the imaginary part of the effective mode index, decreases by only a factor of 10 when the number of rings is increased from 4 to 10. Furthermore, the mode field distribution is always such that the fields fill the entire microstructure, again consistent with the proposition that these are modes of the microstructure as whole. This indicates that the strength of the LPG resonances depends on the number of rings, since the overlap between the fundamental mode localized in the core and the microstructure modes will be weak if the microstructure is very large. By contrast, the LP_{11} mode in the 5th band (mode (b) in Fig. 6) always remains localized in the core and its propagation loss decreases by more than a factor of 10 as each ring is added. If we consider the photonic bandgap model of these PBGFs, mode (b) lies within a bandgap, just like the fundamental core mode, whereas modes (a), (c), and (d) do not. In the case of an infinite structure, the modes of the microstructure become Bloch modes of a photonic band.

Returning to Fig. 5, we note that there is no green curve in the 4th and 6th bands corresponding to an LP_{11}–like core mode. Simulations seem to indicate that, at least for fibers with a single defect core, this mode simply does not exist in the 4th and 6th bands. We have confirmed this not only with careful simulations of fibers with large finite microstructures, but with a fiber having an infinite number of rings using the fictitious source superposition

#10342 - $15.00 USD Received 17 January 2006; revised 9 March 2006; accepted 16 March 2006

method [31]. This is quite an unexpected result, as one would typically assumes that any waveguide structure becomes more strongly multimoded as the wavelength decreases, and so the 6th band should support a HOM in the defect. Furthermore, the blue and red curves in the 5th band appear inverted, with the LP_{12}-like mode of the microstructure having a longer beat length than the LP_{11}-like mode, indicating that the LP_{12}-like mode has a higher n_{eff}. Also, whereas we found that adding more rings causes the real part of the effective index of the microstructure modes to increase in the 4th and 6th bands, adding more rings decreases the mode index the 5th band. The field distribution of these modes in the 5th band, shown in Fig. 7, are actually quite different from those shown in Fig. 6, with very little overlap with the core. More generally, we find that our PBGF has one mode structure associated with the even bands and another associated with the odd bands. For example, the properties of the modes in the 5th band described here also apply to the 3rd and 7th bands. We are currently investigating how this feature relates to the anti-resonant scattering model of PBGFs, and our initial results indicate that the scattering properties of dielectric cylinders do have asymmetries which lead to band parity in solid core PBGFs. This will be described in a future publication.

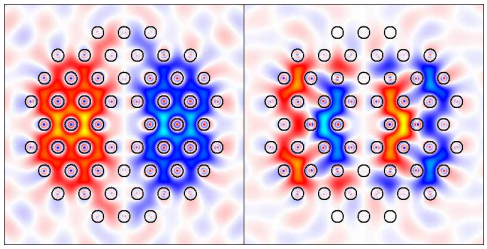

Fig. 7. Simulated transverse mode profiles of LP_{11}- and LP_{12}-like HOMs of the microstructure in the 5th transmission band (985 nm).

5. Conclusion

We have demonstrated the first LPG in a PBGF. The PBGF has a solid core, which allows us to mechanically induce the LPG through periodic stresses. We measure LPG resonances in multiple transmission bands for a single grating period. Numerical simulations of the phase matching condition for the LP_{1x}-like modes of the PBGF are in excellent agreement with the measured resonances. The simulations show that the LPG couples to antisymmetric modes of both the core and the microstructure. The mode structure of the PBGF is quasi periodic in frequency, which allows for coupling to the same mode at multiple wavelengths far from a dispersion turning point; experimentally, we phase match to the LP_{12} mode of the microstructure in both the 4th and 6th transmission bands. We find that in the even bands, one can only phase match to lossy HOMs of the microstructure, whereas in the odd bands, one can phase match to well-confined HOMs of the core as well. This indicates that by adjusting the hole size or index contrast of the PBGF, one fabricate LPGs that act either as mode converters or loss filters at a given wavelength.

Acknowledgments

The authors thank Dr. M. J. Steel and Prof. C. M. de Sterke for many useful discussions. E. D. Moore acknowledges financial support from the University of Colorado Optical Science and Engineering Program (OSEP) and the NSF Integrative Graduate Education and Research Traineeship (IGERT) Program .This work was produced with the assistance of the Australian Research Council under the ARC Centres of Excellence program. CUDOS (the Centre for Ultrahigh bandwidth Devices for Optical Systems) is an ARC Centre of Excellence.